Journal of Magnetic Resonance **151,** 235–241 (2001)
doi:10.1006/jmre.2001.2367, available online at http://www.idealibrary.com on IDEAL®

Phosporus-31 Solid-State NMR in High-Field Gradients: Prospects for Imaging Bone Using the Long Echo-Train Summation Technique (LETS)[1]

D. G. Gillies,* B. Newling,* and E. W. Randall†,[2]

*Department of Chemistry and Department of Physics, University of Surrey, Guilford, Surrey GU2 5XH, England; and †Department of Chemistry, Queen Mary, University of London, London E1 4NS, England

E-mail: e.w.randall@qmw.ac.uk

Received October 6, 2000; revised May 2, 2001; published online July 3, 2001

Stray-field techniques are reported for ^{31}P studies of solids for a variety of compounds including bone, bone meal and calcium hydroxyapatite. Long Hahn echo trains produced by the application of many pulses were used as in the long echo-train summation technique. Double-resonance enhancements of ^{31}P by use of both direct and indirect experiments were attempted on a sample of NH_4PF_6: ^{31}P{^{19}F} double resonance produced, at most, a 26% increase in the initial level of the ^{31}P echo signal. © 2001 Academic Press

Key Words: **phosphorus; bone; stray-field (STRAFI); long echo-train summation (LETS); double resonance.**

INTRODUCTION

There have been myriad studies of solid-state ^{31}P spectra reported in the literature but only a few have dealt with imaging in the solid, despite the interesting possibility of imaging bone. Li reported (*1, 2*) the use of the "solid-echo" method of McDonald *et al.* (*3*) for some one-dimensional profiles of bone. The method uses the Powles–Mansfield solid-echo sequence, $[90^\circ_x–\tau_1–90^\circ_y–\tau_2–\text{echo}]$, and sinusoidal magnetic field gradients. Ackerman *et al.* also used a spin-echo sequence, this time with a low-angle initial pulse and a 180° second pulse, followed by a 180° pulse flip-back, and pulsed field gradients, on a sample of calcium hydroxyapatite, $Ca_{10}(OH)_2(PO_4)_6$, to produce ^{31}P profiles (*4*). Subsequently 3D images were produced by use of a fixed amplitude magnetic field gradient, variation of its direction, and back-projection of the data (*5–8*).

We report the application of the *str*ay-*f*ield (STRAFI) technique to ^{31}P studies of a number of solids with a view to assessing the feasibility of the technique for solid state ^{31}P imaging. The only previous report of ^{31}P STRAFI NMR is by Samoilenko, who obtained a one-dimensional STRAFI image of red phosphorus at 2.9 T and a gradient strength of 37.5 T/m. The image was obtained in less than 1.5 h and had a signal-to-noise ratio of about 25 : 1. The spatial resolution was better than 0.5 mm (*9*).

The STRAFI method employs the large field gradients (58 T/m in this present instance) that occur in the static, stray, or fringe field of superconducting magnets. The quadrature multiple-pulse sequence $[90^\circ_x–(\tau–90^\circ_y–\text{echo}–)_n]$ is usually employed. The short, fixed frequency pulses, usually about 10 μs or less in duration, excite only a narrow slice of the sample because the gradient strength is very large. For protons with relatively narrow lines, the linewidth effect is not the governing factor and the slice thickness is governed by the pulse duration and is about 40 μm for a 10-μs pulse. For other nuclides the slice thickness increases with the ratio of γ_H to γ_X of the observed nucleus, X. This "sensitive slice" can be moved through the sample by translation of the phantom (or adjustment of the excitation frequency) to give a one-dimensional profile. Extension to two and three dimensions may be accomplished by rotations of the sample (*10, 11*) and the technique of back-projection.

The theory and applications of this STRAFI technique, including diffusion aspects, have been reviewed comprehensively by McDonald (*10*), and McDonald and Newling (*11*), and briefly by Randall (*12*). The method, originally due to Samoilenko *et al.* (*13*), has had considerable success for nuclides of all types in virtually any solid, diamagnetic or paramagnetic (*14*), regardless as to whether the nuclide in question is quadrupolar (*9, 14–17*).

The echoes in the echo trains produced by the quadrature sequence above are composite echoes, consisting of the superposition of direct and stimulated echoes, with the number of contributions for any one composite echo depending on the number, n, of pulses used after the first (*18*). The reduction in intensity of the first echo, as the τ-delay is increased, is governed by T_2 only (neglecting diffusion), but subsequent echoes have contributions that have some T_1 character. This T_1 weighting can help give rise to very long echo trains from the extended quadrature sequence $[90^\circ_x–(\tau–90^\circ_y–\text{echo}–)_n]$ because of large values for T_1.

[1] Parts of this work were presented at the 13th International NMR Meeting of the Royal Chemical Society, Exeter, 1997.

[2] To whom correspondence should be addressed. Fax: +44 20 7882 7794.

1090-7807/01 $35.00

For phosphorus 40–60 s is not unusual, for example for bone. Thus this normally bothersome factor becomes a positive aid with this method, since at each spatial location the echoes in each train may be summed to accumulate the signal in the technique of long echo-train summation (LETS). Examples of the use of LETS have been reported recently for ^{2}D (*19*), in both liquid and solid D_2O, and ^{14}N (*20*): values of n in excess of 10,000 have been used, for which gains in the signal-to-noise ratio approaching 100 can be achieved by summation, relative to the $n = 1$ case.

The STRAFI echoes are of the original Hahn type: they are not dipolar (or quadrupolar) in nature, so for example they are produced by liquids, and by solids for virtually any pulse angle and phase (*18, 21, 22*).

In Hahn's original spin-echo experiment, conducted on liquids with arbitrary phase between the 90° pulses, the defocusing (and refocusing) agency was the inhomogeneity of the magnetic field. In the dipolar solid echo, by contrast, it is the dipolar interaction that is the focusing and defocusing factor. The solid echo, unlike the echo in the Hahn case, requires a specific phase relation between the pulses: there must be a 90° phase shift as in the quadrature sequence. The in-phase pulse sequence $[90_x–\tau–90_x]$ produces no dipolar echo. In the STRAFI experiment the dominant interaction is the gradient, as in the original Hahn experiment, despite the dipolar coupling. Consequently no phase shift between pulses is required even for solids: both the quadrature and the in-phase sequences produce STRAFI echoes (*18, 22*). Computer simulations using the Gamma Platform for each of these sequences for a dipolar solid with a 50-kHz dipolar interaction as a function of gradient strength from 0 to 50 T/m reproduce all of these features (*21*).

The STRAFI echoes may be termed state echoes, following Kimmich (*23*), and are independent of the spin–spin variables.

The STRAFI method is very useful for the imaging of heterogeneous solids and liquids in solids, since the susceptibility effects that distort conventional images are very much smaller (*24*).

RESULTS AND DISCUSSION

Table 1 shows the results of the measurements of the ^{31}P relaxation time constants. There are not very large variations in T_2 from sample to sample: the change is only by about a factor of 3, even including the result for the paramagnetic cobaltous phosphate. Variation of T_1 is somewhat larger especially for the cobaltous phosphate, which has a value approximately 100 times shorter than any other. This behavior was expected from previous STRAFI studies of paramagnetic solids (*14*): the paramagnetism shortens mainly T_1, and has only a small effect on T_2, at least at ambient temperatures.

Ackerman *et al.* report a value of 1.8 s at 4.7 T for calcium phosphate, which is rather shorter than the value of 42 s for their ex vivo bone (*7*). The difference was exploited in relaxation weighting experiments (*5*).

TABLE 1
Relaxation Data for Some Solid Phosphorus Compounds at 5.58 T and 96.25 MHz

Sample	T_1 (s)	T_2 (μs)
$Co_3(PO_4)_2$	498×10^{-6}	165
$Ca_3(PO_4)_2$	1.97	443
NH_4PF_6	6.15 (and 6.18*)	232
$AlPO_4$	13.9*	196
Chicken bone	14.7	675
Bonemeal	4.40	481
Apatite (P120)	0.62	448

Note. The values marked * were obtained at 121.5 MHz in the center field of a Bruker MSL 300.

The value of 0.62 s for a sample of calcium hydroxyapatite (P120) in the table is considerably shorter and is the shortest value for the diamagnetic compounds listed. Ackerman *et al.* similarly report a low value of 0.26 s for their sample at 2.0 T (*6*). We may note in passing that a commercial sample of calcium hydroxyapatite proved suspect since it gave very poor ^{31}P STRAFI signals.

The "homogeneous" linewidths derived from the T_2 values in the table are quite modest: the figures for the chicken bone, calcium phosphate, and apatite are each less than 1 kHz. In general the range for bone is generally between 1 and 2 kHz, depending on its provenance (*6*).

Figure 1 shows the STRAFI echo train obtained from cobaltous phosphate. The data shown are the real part of the signals. Short quadrature pulse trains were used, each having a value of

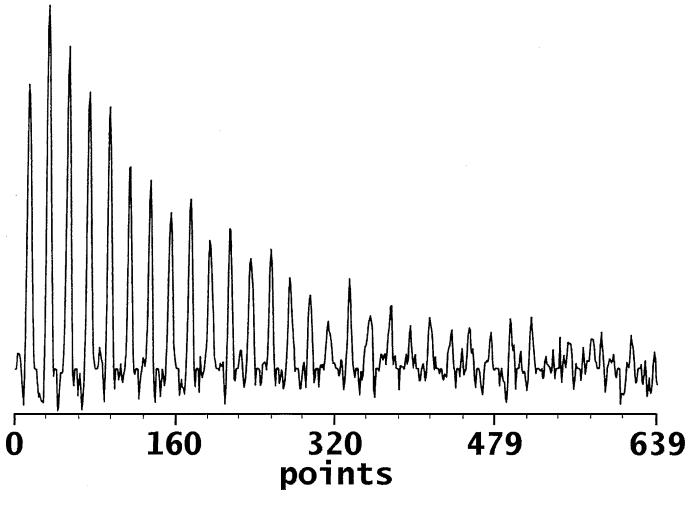

FIG. 1. An example of a typical STRAFI ^{31}P echo train obtained from cobaltous phosphate. The data shown are the real part of the signal: 32 echoes were collected over 1.28 ms at 40-μs intervals (pulse separation, $\tau = 20$ μs) in a total time of 160 s (32 averages, with a pulse delay of 5 s following each acquisition). The amplitude modulation of the echo train, with the first echo attenuated to 2/3 the amplitude of the second, is characteristic of a fringe-field, quadrature echo signal (*25*).

n of 32, giving 32 echoes. Longer echo trains were not feasible. The echoes were collected at 40-μs intervals over 1.28 ms. The value for τ was 20 μs. Thirty-two averages, with a relaxation delay between trains of 5 s, were collected in a total time of 160 s.

Figure 2 shows a quadrature echo train obtained from a sample of chicken bone. The acquisition time for each train of 64 echoes was 5.12 ms, since $\tau = 40\,\mu$s. The total acquisition time was 8.7 h (31 144 averages with a delay between trains of 1 s). The left-hand side of the plot (points 0–1279) shows the real part of the phased data and the right-hand side (points 1280–2559) the imaginary part, which gives an indication of the noise level. The ^{31}P density is sufficiently low in this sample that the acquisition takes considerably longer than for the inorganic sample. In fact the length of time required is at the limits of utility for imaging studies. A striking contrast between Figs. 1 and 2 is the very slow STRAFI decay for the bone sample: the 64th echo is still more than half the intensity of the maximum for the second echo.

The amplitude modulation of the total decay corresponds to the calculations of Benson and McDonald for the quadrature sequence (*25*). They used the Bloch equations and neglected dipolar effects. They also demonstrated the validity of the delta approximation, which treats the pulses as infinitely narrow and of infinite amplitude (but of finite area). Square-pulses in the time domain, when Fourier transformed into the frequency domain, have the form of a sinc function that has side-lobes. In the approximation of a delta-function pulse there are, of course, no relaxation effects during the pulse and the simulated pulses affect a pure 90° rotation, which is certainly not the case experimentally.

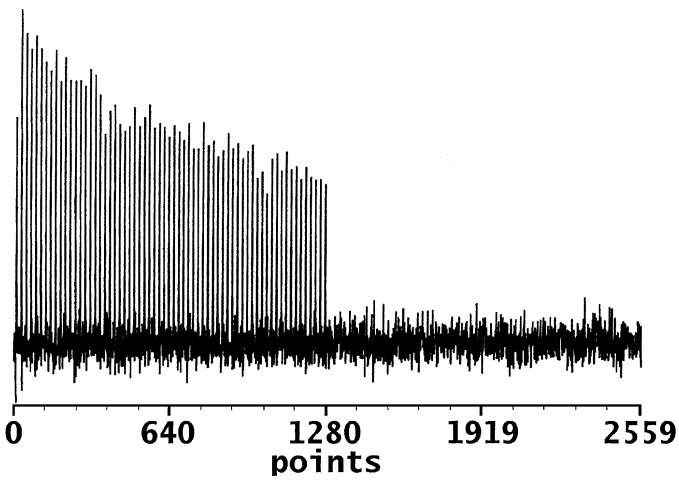

FIG. 2. An echo train obtained from a sample of splintered chicken bone, which had been loosely packed into a 5-mm NMR tube. The train consists of 64 echoes acquired over 5.12 ms ($\tau = 40\,\mu$s). The total acquisition time was 8.7 h (31,144 averages with a pulse delay of 1 s). The left-hand side of the plot (points 0–1279) shows the real part of the phased data and the right-hand side (points 1280–2559) the imaginary part, which gives an indication of the noise level.

Nevertheless the simulation is a very good fit to the experimental data.

The main feature of the modulations in intensity in the echo train is the ratio of intensities of the first four echoes (1 : 3/2 : 3/2 : 11/8). These simulations were reproduced and extended to higher *n* by Bain and Randall (*18*) who used a density matrix approach for a train of 90° pulses applied to "single" spins (again no dipole–dipole interaction), firstly in the absence of a gradient. Relaxation was not included in the simulation. They showed by a consideration of coherence pathways that only a single pathway contributes to the first echo, whereas there are three contributions to the second echo, each 0.5 times the intensity of that giving rise to the first echo. The relaxation of one of these pathways is governed by T_2 alone, whereas in the others the magnetization spends some time stored along the *z* axis and therefore has some additional contribution to its relaxation governed by T_1. There is a fourth term that contributes to the third echo. As *n* increases the number of pathways and the number of contributions to the echoes increase dramatically. The contributions to every composite echo have the same sign for the quadrature sequence, as in constructive interference, whereas there are sign alternations for the in-phase sequence, as in destructive interference. Consequently the in-phase echo train decreases rapidly to 0 with *n*, even though relaxation was not included in the analysis. The quadrature train shows little attenuation with *n*, since relaxation effects were not included. Addition of a gradient to the simulation and summation across the sensitive slice produced little effect, indicating again that the delta approximation is valid.

The rapid attenuation of the STRAFI echo train in Fig. 1 therefore may be attributed to the fact that both T_1 and T_2 are short in this paramagnetic case. Similar effects on the length of echo trains due to paramagnetic influences in shortening relaxation times have been noted before, for example, for ^{2}D in $CuSO_4 \cdot 5D_2O$ (*19*).

Figure 3 shows a more extended quadrature echo train of 8192 echoes obtained from a solid sample of ammonium hexafluorophosphate, NH_4PF_6. These echoes were collected over 360 ms at 44-μs intervals ($\tau = 22\ \mu$s) The total acquisition time for the 512 averages made was 46 min with a delay between trains again set to 5 s. The final echo amplitude in the real part of the signal (points 0–61,439) is significantly greater than the noise level shown in the imaginary part (points 61,440–122,879).

^{31}P Primary Hahn Echoes

Use of the STRAFI technique showed that primary Hahn (or multiple-spin) echoes could be produced easily by solids of all types (*26*). This phenomenon is the production of many echoes from the application of *only two* pulses. We have successfully tested for this effect for ^{31}P in NH_4PF_6. The number of echoes that could be produced, however, was less than 8 for modest accumulation times. The second echo had an intensity only about

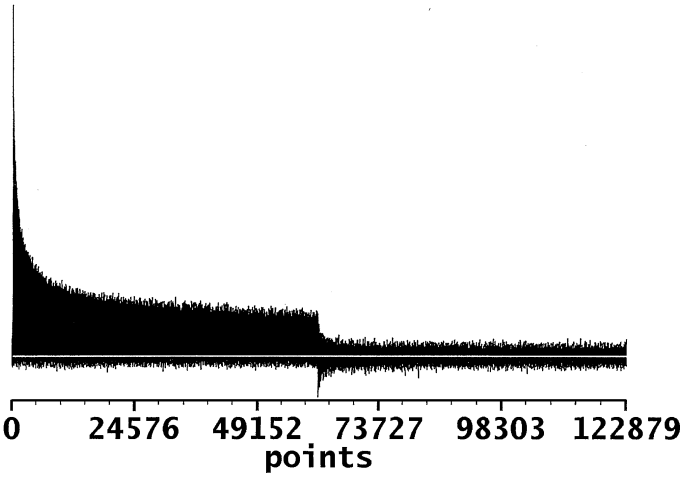

FIG. 3. The extended echo train obtained from ammonium hexafluorophosphate. As many as 8192 echoes were collected over 360 ms at 44-μs intervals ($\tau = 22$ μs). The total acquisition time for 512 averages was 46 min with the relaxation delay set to 5 s. The echo amplitude in the real part of the signal (points 0–61,439) is significantly greater than the noise level (shown in the imaginary part, points 61,440–122,879), even after 360 ms of acquisition.

4% of the first. We may therefore discount this mechanism as a significant contributory cause of the very long echo trains used in LETS.

The phenomenon is caused by the dipolar field, which produces nonlinear effects, because of the breakdown of the high-temperature approximation: the induced field cannot be neglected relative to the Zeeman field.

After the first pulse there is a variation of the tip angle along the gradient direction, and if relaxation is occurring during the pulse there will also be a phase variation. In the vector model the magnetization in the rotating frame consists of an evolving spiral, the pitch of which changes with time. The evolution is reversed by the application of the second pulse and the modulation along the z axis gives the multiple echoes (*27*, *28*).

Spin Locking and T_1 Weighting

Long echo trains are not new in the NMR spectroscopy of solids when the quadrature sequence is used with many pulses. This is the spin-lock sequence that was observed first in 1966 to give line narrowing of dipolar solids by both the Waugh group (*29*) and the group of Mansfield (*30*). Subsequent reports (*31*–*33*) worked out the detailed theory. In the limit of very small τ values the decay of the echo train approximates to $T_{1\rho}$, the relaxation time in the rotating frame. Many echoes, over 2000, were observed.

We may by analogy, therefore, use the idea of spin-locking in the STRAFI experiment to account for the long echo trains obtained even in the presence of a large gradient. In other words the large gradient has the effect of selecting a slice but does not interfere with the spin-lock possibility. Incidentally Kimmich (*23*) has shown that the spin-lock conditions may be used to produce slice selection. We have calculated that with the experimental conditions we use, the gradient-selected slice is much narrower than the slice determined by the spin lock.

In order to account for the form of the decay of the echo train in the STRAFI experiment we may be tempted to invoke the delta approximation and neglect off-resonance effects across the slice. In this case the tip angle does not vary with position across the slice and we may expect a decay of the echo tops that reflects a single relaxation time that approximates to $T_{1\rho}$.

In fact we know that the tip angle changes markedly across the slice as witnessed by the observation of primary Hahn echoes. Rhim *et al.* (*34*, *35*) established that spin-locking can occur with any tip angle, α, with the multiple-pulse train $[\alpha_x\text{–}(\tau\text{–}\alpha_y\text{–echo–})_n]$. In fact longer echo trains were produced for $\alpha = 45^\circ$ than for $\alpha = 90^\circ$, although of course the initial magnetization was less. Using this model we may expect an exponentially decaying echo train from *each position in the slice*, the initial magnetization and the time constant varying with position as the tip angle changes. In this case we expect the observed echo train to be the sum of many different exponentials. Our results show that the STRAFI decay is not a single exponential.

An alternative or parallel idea for long trains is the T_1-weighting hypothesis resulting from the analysis of the coherence pathways (*18*). This is supported by the empirical observation that samples with long T_1 values give long STRAFI echo trains.

Unfortunately there are no published simulations so far of the relaxation attenuation of STRAFI echo trains caused by inclusion of relaxation times in the treatment.

Long Echo-Train Summation

Because of the large bandwidths in imaging work on solids, the signal-to-noise ratios are relatively poor, and means of signal enhancement are highly desirable, additional to the conventional accumulation of echo trains. It has always been normal in STRAFI imaging to sum the tops of echoes in each echo train. Rarely, however, has it been the practice to record and sum more than about 32 echoes in any one train.

The realization that very long echo trains ($n > 1000$) could be used came first with the STRAFI-work on deuterium (*19*) and the ^{31}P work now presented here. The phenomenon, though, is quite general and occurs even for the quadrupolar nuclide ^{14}N, for which large electric quadrupole couplings may be present (*20*). Early STRAFI work on ^{11}B (*36*) has now been extended to include very large values of n (*37*).

Figure 4 illustrates the utility of the method, now referred to as LETS for ^{31}P. It shows a one-dimensional profile of a sample of ammonium hexafluorophosphate contained in a cylindrical NMR tube of 5 mm diameter. The probe was lowered manually in the field gradient in crude steps of 0.35 mm through the sensitive slice. At each position 64 echo trains were summed with a relaxation delay between trains of 5 s. The acquisition time

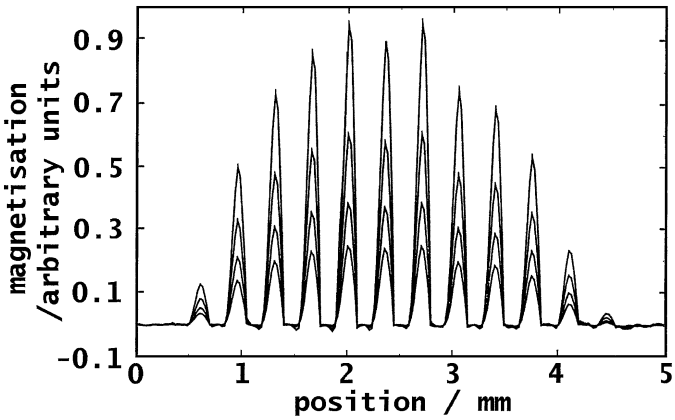

FIG. 4. A profile of a 5-mm NMR tube packed with ammonium hexafluorophosphate. The probe was lowered manually, in steps of 0.35 mm, through the sensitive slice. At each position, an echo train like that shown in Fig. 3, was collected, but the number of signal averages were reduced to 64, bringing the acquisition time at each position down to 5.7 min. The RF pulses had a duration of 3.5 μs, which excited a 0.28-mm (277-kHz) slice. Some of the 8192 echoes were then summed to give a single echo-envelope representative of the ^{31}P signal available at that position. Four such echo sums are shown at each position in the profile, resulting from summation of the first 8192, 4096, 2048, and 1024 echoes in the train (top to bottom).

for each slice was 5.7 min. Each pulse had a duration of 3.5 μs, which excited a slice of width 0.29 mm. The frequency spread across the slice is 277 kHz. From the T_2 value in Table 1 we may calculate the homogeneous linewidth as less than 1.5 kHz, so that we may neglect the linewidth effect on the resolution. Better spatial resolution could of course be accomplished by reduction of the step-size and lengthening the pulse duration. A resolution of better than 100 μm is thus feasible.

Some of the 8192 echoes were then summed to give a single echo-envelope representative of the ^{31}P signal available at that position. Four such echo sums are shown in Fig. 4 at each of the 12 positions resulting from summation of the first 1024, 2048, 4096, and 8192 echoes in the train respectively (from bottom to top).

It is clearly apparent that the use of LETS gives a pronounced enhancement. Relative to the signals for the bottom set with 1024 echoes, the signals for the three other values of n give enhancements that are approximately $0.75\sqrt{n}$.

One strategy in conventional STRAFI imaging is to acquire one echo train at each position, translate the sample, and accumulate subsequent averages on subsequent passes through the sample positions. This interleaving allows spin–lattice relaxation for any one slice to occur during the sample motion, which is normally slow, about 1 s, for a complete pass of a few millimeters. The idea is to avoid lengthy relaxation delays. Because of the long T_1 values for many solids, such as bone, for which T_1 may be as long as 60 s, this is not a viable strategy. The LETS method provides an advantageous alternative, since it makes a merit of the long T_1values. Moreover signal loss due to T_2, for example, between the first two pulses is not a major difficulty since the T_2 values are not very short for the phosphorus compounds we have investigated.

It appears that LETS is a strategy that can be applied advantageously in studies of bone. The occurrence of long echo trains for chicken bone is shown in Fig. 5. As many as 4096 echoes were acquired over 180 ms ($\tau = 22$ μs). The total acquisition time was 1.28 h (891 averages with a delay between pulse trains of 5 s). The echo amplitude after 180 ms is a significantly greater proportion of the initial signal level for the chicken bone than for the ammonium hexafluoride sample in Fig. 3 (0.27 vs 0.13).

Double Resonance

The aim of the double-resonance studies was to determine conditions under which signal enhancement could be obtained. There are no reports of similar attempts in STRAFI experiments. Successful ^{1}H–^{31}P cross-polarization imaging experiments on chicken bone at 6.0 T in modest gradients (<100 G/cm) have been reported by the Ackerman group, which gave time-savings by about a factor of about 20 (*5*).

Ammonium hexafluorophosphate was the main sample used in this part of our study. It was chosen as a favorable model compound because the close proximity of the two types of nucleus, ^{19}F and ^{31}P, ensures a larger dipolar interaction than the ^{1}H–^{31}P interaction in bone (~1–2 kHz). The P–F internuclear distance is 1.58 Å, which yields a dipolar interaction of about 12 kHz. In fact one may expect some line narrowing because of rotation of the PF_6 anion. The indirect coupling is reported to be 743 ± 12 Hz (*38*).

In general double-resonance experiments require the matching of the two frequencies that here are for the ^{19}F and ^{31}P transitions. In STRAFI this requires that the two sensitive planes (excited slices) overlap. This may be attained by adjustment of the two freqencies. It is also desirable that the two slice thicknesses

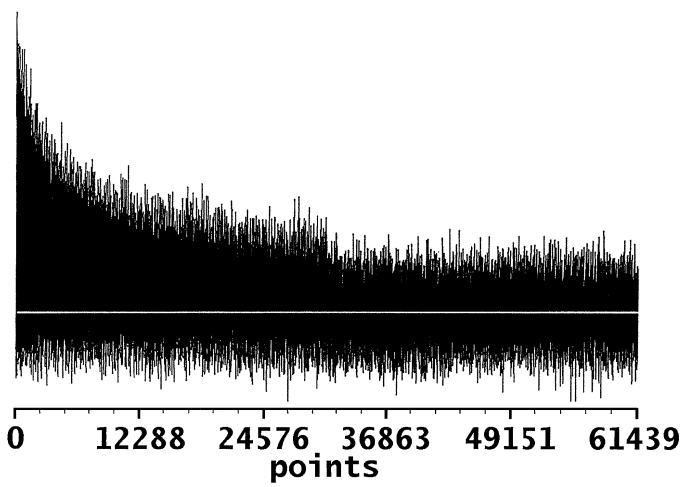

FIG. 5. Long echo trains from chicken bone. The real part of the signal is on the left and the imaginary part is on the right. In each train 4096 echoes were acquired over 180 ms ($\tau = 22$ ms). There were 891 averages with a relaxation delay between trains of 5 s. The total acquisition time was 1.28 h.

should be the same. This condition may be met by adjustment of the powers of the two Rfs. Relative to the spectroscopic situation, where $G = 0$, one degree of freedom has been lost.

The envelope of the decay of the echo amplitude in a fringe-field ^{31}P long echo train may be represented approximately by a single exponential decay plus a constant to account for an effect analogous to spin-locking. In the case where $\tau = 30$ μs and 256 echoes were collected, a typical decay time constant, which probably lies somewhere between T_2 and $T_{1\rho}$, is 4.09 ms. The amplitude of the constant comprises 21% of the total initial signal amplitude. An echo train collected after ^{19}F presaturation shows an initial decay constant of 4.02 ms and the constant is 22% of the total initial signal amplitude. The total signal amplitude is increased by 26%.

In an experiment in which simultaneous quadrature echo trains were applied to both ^{19}F and ^{31}P, the envelope may again be represented by a single exponential decay plus an offset ($\tau = 30$ μs, 256 echoes were collected). With $B_{1F} = 0$, the decay time constant is 3.71 ms and the constant comprises 16% of the total initial signal amplitude. Under the Hartmann–Hahn condition, the decay time is 3.35 ms, but the constant accounts for only 7.3% of the total amplitude. There is a 16% increase in total initial signal amplitude. These effects upon the ^{31}P echo train are canceled if the frequency of the^{19}F excitation is moved sufficiently far (7 MHz) off resonance.

It is clear that the presaturation method gives the more favorable result, for use in conjunction with the LETS approach. Although the gains are modest so far, they are nevertheless useful if employed together with LETS. The use of other double-resonance methods failed to produce any change in the ^{31}P signal, at least in our hands.

CONCLUSIONS

LETS is a practical and easily implemented strategy for the enhancement of ^{31}P signals in bone and other phosphorus-containing solids. Considerable reductions in imaging times should be possible with its adoption. For example Samoilenko's ^{31}P 1D STRAFI projection (*9*), which took less than 1.5 h, was accomplished with only 48 echoes in each echo train. LETS could reduce this time by a factor of at least 10 to say 10 min. Extension of the dimensionality from 1D to 3D might be feasible. In this case Samoilenko's sample of red phosphorus is of course particularly favorable in terms of nuclear density—bone is less favorable in this regard. The T_1 values of red phosphorus and many bones are comparably long.

Although the enhancements resulting from saturation of the ^{19}F transitions are modest, they are nevertheless useful in conjunction with the LETS technique.

One great advantage of the STRAFI method for the imaging of inhomogeneous solids is that the magnetic susceptibility effects that distort conventional NMR images are very much smaller because of the large size of the STRAFI gradients used (*24*). This is particularly important if there are paramagnetic or metallic centers in the phantom.

The large gradients also improve the spatial resolution in proportion to G. This factor is particularly welcome for samples that have small values of T_2 since these require the use of short echo times, which reduce the resolution: a higher gradient can offset this disadvantage. In addition, a constant gradient technique such as STRAFI does not suffer from the time wasted waiting for the decay of eddy currents in switched gradient experiments.

Crystalline samples are accessible by STRAFI NMR, which can deal with very short relaxation times, shorter than those accessible by other MRI techniques. For samples with longer T_2 values the spatial resolution may be improved by the use of longer values for τ than those used here.

Phosphorus STRAFI techniques therefore are potentially useful in a number of areas, additional to the study of bone and bone marrow, such as implants and dental materials, and for environmental studies involving phosphorus in soils and rocks. They may, however, be restricted to studies in one dimension because of the time factor.

EXPERIMENTAL

The spectrometer was a Chemical Magnetics Infinity System (Varian U.K., Solid State Office, Harrogate, U.K.) with a Magnex superconducting solenoid of central field 9.4 T (Magnex Scientific Limited, Oxfordshire, UK). The stray field utilized was in the region of 5.58 T for which the ^{31}P resonance frequency was 96.25 MHz and the ^{1}H frequency 237.5 MHz. The STRAFI gradient strength was 58 T/m. The STRAFI probe-assembly consisted of a Bruker CXP 200 probe with a homebuilt horizontal solenoid and sampling positioning assembly. The horizontal coil was of length 18 mm with an internal diameter of 5 mm and 14 space-wound turns.

Samples studied include cobaltous phosphate, $Co_3(PO_4)_2 \cdot 8H_2O$, calcium phosphate, $Ca_3(PO_4)_2$, ammonium hexafluorophosphate, NH_4PF_6, bone meal (ingredients listed included "17% P_2O_5"), chicken bone, and two samples of calcium hydroyapatite, $Ca_9(PO_4)_6 \cdot Ca(OH)_2$, a commercial sample (Aldrich) and one synthesied by Dr. Isaac Abraham (P120). The bone was splintered into small slivers, whereas the other solids were used as powders. Samples were packed in NMR tubes of 5 mm diameter cut down to about 20 mm in length.

The extended quadrature sequence, $[90^\circ_x$–$(\tau$–90°_y–echo–$)_n]$, was used to produce long echo trains. The delay between trains generally was on the order of T_1 or less, and acquisitions were, therefore, performed under a steady state regime. Calibration of the tip angle was accomplished with the in-phase sequence, $[90^\circ_x$–$(\tau$–90°_x–echo–$)_n]$, which produces Rabi-like alternation of echo-intensities (*39*) or by measurement of the ratio of echo heights in the quadrature sequence (*25*).

Relaxation measurements in STRAFI experiments were by the saturation recovery technique for T_1, with saturation being accomplished by a series of 90 pulses with decreasing

separation. T_2 was measured by observation of the intensity of the first echo as τ was increased in the quadrature sequence. Other ^{31}P relaxation measurements were made at the central field of a Bruker MSL300.

In the double-resonance work the RF coil was doubly tuned using a lower frequency of 86.7 MHz for ^{31}P and 201.5 MHz for ^{19}F. The exact frequencies were chosen so that the ^{31}P and ^{19}F sensitive planes were coincident for a sample of NH_4PF_6 (according to literature values for chemical shifts). The pulse durations used were in the inverse ratio of the magnetogyric ratios, so that the two sensitive planes were of the same spatial width. This is equivalent to the traditional Hartmann–Hahn match condition (being governed by the ratio of magnetogyric ratios). Several double-resonance methods were employed. In the simplest, the ^{19}F resonance was saturated (see below) prior to acquisition of a ^{31}P quadrature echo train. Other methods included quadrature echo pulse trains applied to both ^{31}P and ^{19}F simultaneously, and traditional cross-polarization experiments (with the cross-polarization attempted adiabatically or by the use of a series of discrete RF pulses) (*40*).

ACKNOWLEDGMENTS

We are very grateful to Dr. J. Godward for spectral assistance, to R. Lane and B. Smethhurst for construction of the assembly for sample positioning, to Dr. I. Abraham for the P120 sample, and to Professor A. Samoilenko for useful discussions. Thanks are due also to Dr. Abil Aliev at the University of London's MSL 300 Intercollegiate service situated at University College, and to Dr. N. Mahieu for assistance with the figures. The work was supported by EPSRC Grant GR/K 12397.

REFERENCES

1. L. Li and R. A. Kruger, *Phys. Med. Biol*. **35,** 1153–1158 (1990).
2. L. Li, *Phys. Med. Biol*. **36,** 199–206, 1127–1132 (1991).
3. P. J. McDonald, J. J. Attard, and D. G. Taylor, *J. Magn. Reson*. **72,** 224–229 (1987).
4. J. L. Ackerman, D. P. Raleigh, and M. J. Glimcher, *Magn. Reson. Med*. **25,** 1–11 (1992).
5. J. R. Moore, L. Garrido, and J. J. Ackerman, *Magn. Reson. Med*. **33,** 293–299 (1995).
6. Y. Wu, J. L. Ackerman, D. A. Chesler, J. Li, R. M. Neer, J. Wang, and M. J. Glimcher, *Calcif. Tissue Internat*. **62,** 512–518 (1998).
7. C. Ramanathan and J. L. Ackerman, *Magn. Reson. Med*. **41,** 1214–1220 (1999).
8. Y. T. Wu, D. A. Chesler, M. J. Glimcher, L. Garrido, J. X. Wang, H. J. Jiang, and J. L. Ackerman, *Proc. Natl. Acad. Sci. USA* **96,** 1574–1578 (1999).
9. A. A. Samoilenko, *in* "Proceedings of the 28th Congress Ampere" (M. E. Smith and J. H. Strange, Eds.), pp. 139–140, University of Canterbury (1996).
10. P. J. McDonald, *Prog. NMR* **30,** 69–99 (1997).
11. P. J. McDonald and B. Newling, *Repts. Prog. Phys*. **61,** 1441–1493 (1998).
12. E. W. Randall, *in* "Encyclopaedia of Spectroscopy and Spectrometry" (J. C. Lindon, Ed.), pp. 1396–1403, Academic Press, San Diego (2000).
13. A. A. Samoilenko, D.-Yu Artemov, and L. A. Sibel'dina, *JEPT Lett*. **47,** 417–419 (1988).
14. E. W. Randall, A. A. Samoilenko, and T. Nunes, *J. Magn. Reson. A* **116,** 122–124 (1995); E. W. Randall, *Solid State NMR* **8,** 173–178 (1997).
15. E. W. Randall and D. G. Gillies, *J. Magn. Reson. A* **121,** 217–220 (1996).
16. P. Bodart, T. Nunes, and E. W. Randall, *Solid State NMR* **8,** 257–263 (1997).
17. P. Bodart, T. Nunes, and E. W. Randall, *Applied Magn. Reson*. **12,** 269–273 (1997).
18. A. D. Bain and E. W. Randall, *J. Magn. Reson. A* **123,** 49–55 (1996).
19. E. W. Randall, T. G. Nunes, G. Guillot, and P. R. Bodart, *Solid State NMR* **14,** 165–172 (1999).
20. E. W. Randall, A. A. Samoilenko, and R. Fu, *Solid State NMR* **14,** 173–179 (1999).
21. S. A. Smith and E. W. Randall, Poster at the 29th Ampere–13th ISMAR Conference, Berlin, 1998; Annual Report for 1998, pp. 252–253, The National High Magnetic Field Laboratory, Tallahassee, 1999.
22. E. W. Randall, A. A. Samoilenko, and T. Nunes, *Quart. Magn. Reson. Biol. Med.* **2,** 299–300 (1995).
23. R. Kimmich, "NMR, Tomography, Diffusometry, Relaxometry," Springer-Verlag, Berlin (1997).
24. P. Kinchesh, E. W. Randall, and K. Zick, *J. Magn. Reson.* **100,** 411–415 (1992); and *Magn. Reson. Imaging* **12,** 305–307 (1994).
25. T. Benson and P. J. McDonald, *J. Magn. Reson. A* **112,** 17–23 (1995).
26. E. W. Randall, A. A. Samoilenko, and T. Nunes, *J. Magn. Reson. A* **116,** 259–261 (1995).
27. R. P. O. Jones, G. A. Morris, and J. C. Waterton, *J. Magn. Reson.* **98,** 115–122 (1992).
28. R. Bowtell, R. M. Bowley, and P. Glover, *J. Magn. Reson*. **88,** 643–651 (1990).
29. E. D. Ostroff and J. S. Waugh, *Phys. Rev. Lett*. **16,** 1097–1098 (1966).
30. P. Mansfield and D. Ware, *Phys. Lett.* **22,** 133–135 (1966).
31. J. S. Waugh and C. H. Wang, *Phys. Rev.* **162,** 209–216 (1967).
32. P. Mansfield and D. Ware, *Phys. Rev.* **168,** 318–334 (1968).
33. P. Mansfield, K. H. B. Richards, and D. Ware, *Phys. Rev. B* **1,** 2048–2063 (1970).
34. W.-K. Rhim, D. P. Burum, and D. D. Elleman, *Phys. Rev. Lett.* **37,** 1764–1766 (1976).
35. W.-K. Rhim, D. P. Burum, and D. D. Elleman, *J. Chem. Phys.* **68,** 692–695 (1978).
36. D. G. Gillies and E. W. Randall, *J. Magn. Reson. A* **121,** 217–220 (1996).
37. D. G. Gillies, J. Godward, and E. W. Randall, in preparation.
38. R. Challoner, T. Schaller, and A. Sebald, *J. Magn. Reson. A* **101,** 106–108 (1993).
39. E. W. Randall, *Solid State NMR* **8,** 179–183 (1997).
40. N. Chandrakumar and R. Kimmich, *J. Magn. Reson.* **137,** 100–107 (1999).